Construction of an inexpensive surface plasmon resonance instrument for use in teaching and research

Barry K. Lavine *, David J. Westover, Leah Oxenford, Nikhil Mirjankar, Necati Kaval

Department of Chemistry, Oklahoma State University, Stillwater, OK 74078-3071, USA

Abstract

The construction of an inexpensive SPR instrument that can be used for both teaching and research is described. Using a $2' \times 2'$ optical table to construct this instrument allows both scientists and students full access to the operation of the spectrometer. Furthermore, the use of open platform instrumentation has the advantage of maintaining the focus on the relationship between emerging technology and analytical chemistry as well as allowing the user to modify the instrument to enhance the measurement process for a particular application. This is a change from the learning paradigm used in most research and teaching laboratories where commercial instrumentation is treated as a black box due to its complexity. Three studies, which were performed using this instrument, are presented to demonstrate the suitability of this instrument for both teaching and research. These studies include measuring the refractive index of alcohols, investigating the partitioning of ruthenium (II) trisbipyridine chloride into Nafion, and understanding the mechanism controlling metal ion adsorption by polyacrylamide hydrogels.
© 2007 Elsevier B.V. All rights reserved.

Keywords: Surface plasmon resonance; Refractive index; Evanescent wave techniques; Thin films; Chemical education

1. Introduction

Surface plasmon resonance (SPR) spectroscopy is a technique that can detect changes of 10^{-4} to 10^{-5} refractive index (RI) units within approximately 200 nm of the SPR surface/sample interface. Because the deposition of a 0.01 nm film corresponds to an RI change of 0.1 RI units [1], SPR has been used to study thin films deposited on sensing layers [2]. Currently, SPR is being used as a sensitive refractometer for refractive index measurements in process control and analytical chemistry [3]. Perhaps the most well documented application of SPR is the characterization of antigen–antibody interactions [4].

All SPR spectrometers have a laser, detector, and a glass prism in contact with a thin metal layer usually gold. SPR instruments employ either angle scanning or wavelength scanning to collect spectra. Angle scanning instruments are the most popular. The wavelength of the light source is held constant and the angle of incidence is varied. Wavelength scanning

instruments, on the other hand, create resonance by fixing the incident angle while changing the wavelength of the light source.

The introduction of SPR and other evanescent wave techniques into the teaching and research laboratory is advantageous for several reasons. Undergraduates benefit from the opportunity to work with modern instrumentation that can be used to study chemical events occurring at interfaces. Furthermore, student interest in modern chemical instrumentation can lead to their participation in long-term undergraduate research projects. For the researcher, the most significant advantage of SPR is label free detection [5]. The combination of SPR and electrochemistry to study surface processes is very attractive since the noble metal layer used to excite plasmons can also be used as the working electrode [6].

Despite all of these advantages, SPR is currently not found in most research or undergraduate teaching laboratories because of the sheer cost of a commercial instrument, which is prohibitive for most teaching and research laboratories in colleges and universities. The most successful commercial SPR systems are the BIAcore systems which sell for $300,000.00 [7]. In this article the construction of an inexpensive SPR (angle scanning) instrument that can be used for both teaching and research is

---

* Corresponding author.
 E-mail address: bklab@chem.okstate.edu (B.K. Lavine).

described. Using a $2' \times 2'$ optical table to construct this instrument allows both scientists and students full access to the operation of this system. Furthermore, the use of open platform instrumentation has the advantage of maintaining the focus on the relationship between emerging technology and analytical chemistry as well as allowing the user to modify the instrument to enhance the measurement process for a particular application. This is a change from the practice adopted in most research and instructional laboratories where commercial instrumentation is treated as a black box, and scientists and students using this type of instrumentation are only concerned with reporting results [8]. Three studies, which were performed using this instrument, are presented to demonstrate the suitability of this instrument for both teaching and research.

2. Theory

Surface plasmon resonance is a charge density wave phenomenon that arises at the surface of a metallic film. It occurs in the visible and near infrared regions in free electron metals such as silver and gold. Regions of high and low electron density are created which propagate along the surface.

Surface plasmons cannot be directly excited by striking the metal surface with an incident beam of photons. However, excitation of surface plasmons can be achieved using an evanescent wave created from plane polarized light that passes from a medium of high refractive index to a medium of low refractive index at an incident angle greater than the critical angle. Resonance occurs when the x component of the incident wavevector k refracted into the metal (i.e., the evanescent wavevector $\vec{k}_e$) is equal to the x component of the surface plasmon wavevector $\vec{k}_s$. By changing the incident angle, one can vary the evanescent wavevector $\vec{k}_e$ until it matches $\vec{k}_s$.

The use of an evanescent field to generate surface plasmon waves was first introduced by Kretschmann and is referred to as the Kretschmann configuration [9]. He proposed applying a nano-thin gold surface on the base of a right angled prism with the sample in contact with the gold. Plasmon resonance is then detected by projecting light into the prism at various angles and measuring the intensity of the light reflected.

The angle at which the reflected light intensity is at a minimum is the angle of maximum plasmon resonance. Fig. 1 shows an SPR spectrum obtained by measuring the intensity of the light reflected internally within a right-angle prism as a function of the incident angle. The primary attributes of this spectrum are the angle at which minimum reflectance intensity or resonance occurs (see B in Fig. 1), and the critical angle, where total internal reflection is initiated (see A in Fig. 1). The resonance angle strongly depends on the refractive index profile of the sample in the evanescent field which is located within 200 nm of the metal surface. Any changes in the optical properties of this region will influence both the resonance angle and the shape of the SPR curve. This is the basis of SPR [10]. At the resonance angle, the energy of the incident photon is completely transferred to electrons in the metal. For chemical analysis, this can be very attractive because the measured physical quantity is a refractive index change. No chromophoric group or labeling of the molecule is required.

There are other instrumental configurations that utilize evanescent waves to excite surface plasmons. The Otto configuration [11], which also utilizes attenuated total reflectance, imposes a dielectric (sample) between the right angle prism and metal layer. Maintaining a constant distance between the prism and the metal layer at some specified value can pose problems. Because the evanescent wave must traverse the sample in order to generate the surface plasmon wave, photon absorption by the sample can occur reducing the reflected light
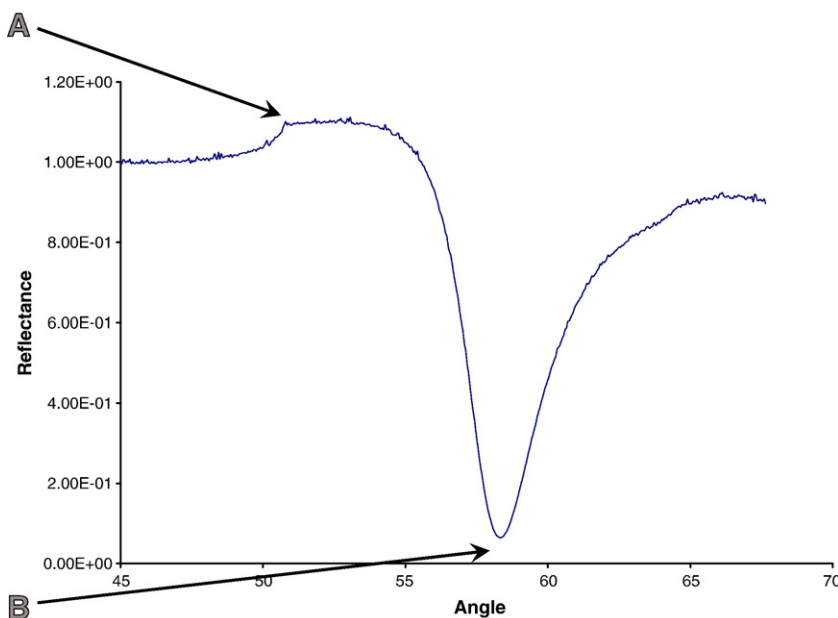
Fig. 1. An idealized SPR spectrum. The critical angle (A) and the resonance angle (B) are labeled.

intensity. Other configurations involve gratings which have been substituted for right angle prisms but the sensitivity of SPR sensors based on gratings is less than SPR devices that utilize prism couplers [12]. Fiber optic SPR has recently attracted considerable attention [13–16]. Single mode optical fibers with a portion of the cladding removed and a metal layer deposited around the exposed section of the fiber core have been used to generate a plasmon field. However, only wavelength scanning is possible since the incident angle within the fiber cannot be varied. In addition, the operating range of the optical fiber for wavelength is limited. Nevertheless, the use of optical fibers for SPR is advantageous since it allows for the construction of miniaturized sensors that can be deployed in the field.

3. Instrumental design

The basic design of the open platform SPR instrument, which utilizes a Kretschmann configuration, is shown in Fig. 2. Angle scanning is performed by measuring the reflected light intensity as the prism and the detectors are rotated. The basic components of this instrument, which can be purchased from any optics distributor, include a low power laser (635 nm, 3 mW), two detectors (reference and primary), a polarizer, a beam splitter, and two rotation stages with the optics mounted on top. A detailed listing of the parts is included in the supplemental material. Any laser with a wavelength greater than 550 nm can be used to generate plasmons in gold, but a communication grade diode laser is preferred because of cost. If the wavelength of light is less than 550 nm, photons will be absorbed by the gold via electron excitation. This removes electrons from the conductance band preventing the formation of plasmons. Longer wavelength lasers are generally preferred because the thickness of the plasmon field generated is proportional to the wavelength of light used to energize the metal.

A simple glass polarizer is used to enhance the overall SPR signal by removing light generated by the laser that is not polarized parallel to the plane of incidence. After the light passes through the polarizer, a fraction of the laser beam is reflected away from the main beam path by a beam splitter, which in this instrument is a hand polished glass slide. The fraction of light diverted away from the main beam goes to the reference detector, which is a solid state silicone detector. The silicon detector generates a voltage proportional to the light intensity. This voltage when divided into the voltage reading from the primary detector normalizes the laser intensity thereby removing noise caused by power fluctuations in the laser output.
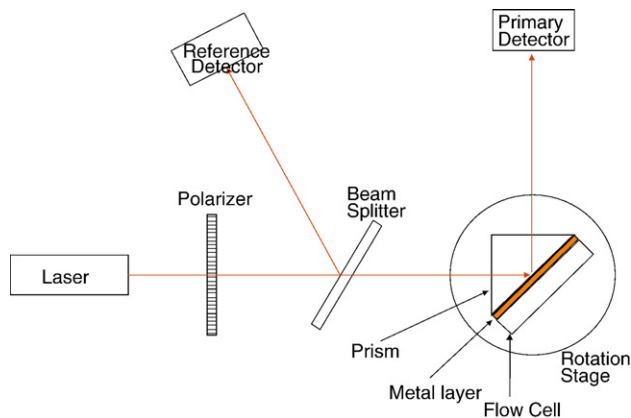
Two identical rotational stages mounted independently of each other are controlled by Lab View software (National Instruments, Austin, TX). An SF10 right angle prism (through which the laser light generates an evanescent field) and an optically matched SF10 glass slide coated with gold and a liquid sample holder are mounted on the top rotation stage. SF-10 is desirable because the index of refraction ($n = 1.72$ at 635 nm) is large enough to allow for SPR measurements of aqueous samples. The bottom rotation stage, which controls the rotation of the primary detector, is programmed to rotate at twice the rate of the top (optical) stage. Both stages utilize a worm drive that rotates the table 1° for 96 full steps of the stepping motor. This defines the accuracy of the instrument which is approximately ±0.01° for both the resonance and critical angle.

A flow cell with a 0.28 ml volume is incorporated into the instrument because it allows for constant flow of sample analyte to the gold surface allowing multiple experiments to be performed consecutively. The sample solution can be introduced to the gold surface by manual injection or by a syringe pump. The flow cell is made of Plexiglas, which is a clear plastic. Its front face has a 1/16″ deep and 1/2″ wide circular well with inlet and outlet holes located at the bottom and top of the well. The front face is mounted on the flow cell using two fastening screws. An O-ring slightly thicker than the depth of the well is also used in order to ensure that the cell is leak proof. Teflon tubing is connected to the entrance and exit ports on the back of the flow cell. The cell, which is fixed on a small aluminum plate for ease of handling, is mounted on the top rotation stage. An aluminum front face with a vertical 90° V-grove is used to fasten the prism and gold coated slide to the flow cell, with the right angle prism firmly placed in the V-grove. A 0.5″ by 1″ SF10 gold slide is directly coupled to the prism using an index matching fluid (Cargille Laboratories Series M certified 1.725 refractive index matching fluid, Cargille Labs, NJ), which effectively makes the gold slide an integral part of the prism. Care must be taken not to expose the gold side of the slide to the index matching fluid. Additional information about the flow cell is included in the supplemental material.

Once the cell has been fastened together, it is mounted on a small x–y translation stage on the top rotation stage. During the initial alignment, the cell is moved back and forth using the translation stage to position the laser beam and the center of the gold slide on the center of the rotation axis. Since the cell is made of Plexiglas, the laser beam, which is passing through the prism and hitting the gold surface, can be monitored visually during the alignment.

To complete the instrument, a number of mounting components need to be fabricated. Detailed drawings for all of the mounting components are also included in the supplemental

Fig. 2. Block diagram of the SPR instrument described in this paper.

material. The instrument is housed on a standard optical table using standard mountings, except where specified, and the distance between the laser and the prism is 35 cm. The electronics for the motor control unit and A/D converter which were assembled as described in the schematic are found in the supplemental material. The housing will need a power cord, on/off toggle switch, and four external connection ports. In addition, there should be a power supply for the motors and a fuse for the entire system. When constructing the control unit, the housing and power supply should be well grounded as this can be a major source of background noise. All electronic components were purchased from DigiKey (Thief River Falls, MN). The A/D converter was purchased from National Instruments (Austin, TX).

4. Data analysis

Two different software packages were used to process the SPR data. The first is LabView Full Development System (National Instrument, Austin, TX), which controls the motors as well as collects and saves the spectrum from the detectors. The signal from the two detectors is divided (primary/reference) and normalized to the first data point. This minimizes laser source intensity variation in the data allowing the spectra to be set to the same scale. SPR spectra are saved as ASCII files for transfer to other programs for additional data processing.

The second software platform used was MATLAB (The Mathworks, Inc. Natick, MA). Each spectrum imported into MATLAB was first corrected for the refraction of the laser light entering into the prism. Each corrected spectrum was run in a model-matching program that was developed in house. The program uses Fresnel's equations to build a four-layer or five-layer model from which the actual physical parameters of the system can be determined from the model/data fit. The MATLAB program allows the operator to vary the main parameters from their ideal setting to alter the spectrum. Variables that can be altered by the operator include the wavelength of the laser, refractive index of the prism (ε_0), which is layer 0, real dielectric coefficients (ε_1^r, ε_2^r, ε_3^r, ε_4^r), imaginary dielectric coefficients (ε_1^i, ε_2^i, ε_3^i, ε_4^i), and the thickness (d_1, d_2,

d_3, and d_4) of layers 1, 2, 3, and 4. As shown in Fig. 3 for a four-layer model (layers 0, 1, 2, and 3), layers 1 and 2 are designated as the chromium (adhesion layer) and gold layers. In a typical SPR experiment, an SPR slide is first tested in air (constant index of refraction, $n = 1.0002$), allowing for the parameters of the gold and chromium layers to be determined. This is necessary since no two slides will have the same exact values because they will not possess the same degree of uniformity for their chromium and gold layers. These values will be fixed for all studies carried out with this slide.

5. Experimental

5.1. Optical alignment

The optical alignment of the open platform instrument is a straightforward task. Although the plasmon wave can be detected with minimal alignment, correct alignment is crucial to accurately measure the refractive index of the sample layer. The center of the top (optical) rotational stage should be in line with the laser beam, with the prism rotated such that its entrance face is both perpendicular and level to the laser. To ensure that the prism's surface is perpendicular to the laser, an index card can be used to locate the reflected light from the prism. If the prism is properly aligned, the reflected beam will return to the source. Determining the alignment for the other optical components can be achieved by placing a card directly in front of the prism. If all of the optical components are correctly aligned, no stray reflections will be evident in the vicinity of the primary beam. If stray reflections occur, it will be necessary to realign the different optical components until all stray points coincide with the main beam. Caution should be taken with the positioning of the detectors during the alignment procedure. A small amount of light will be reflected off of their surface. To minimize this stray light, the detectors should be positioned at an angle such that reflected light from them will not strike any of the other optical components.

5.2. Preparation of gold slides

SF10 slides ($3'' \times 1''$) were purchased from Esco (Oak Ridge, NJ). The slides were placed in a piranha solution (two parts conc. nitric acid and one part 30% hydrogen peroxide) for 1 h. Each slide was rinsed thoroughly with distilled water, followed by an ethanol rinse, and dried with nitrogen gas. Using a vapor deposition chamber, a thin layer of chromium (1 nm) followed by gold (50 nm) was deposited onto each slide. (Chromium is used as an adhesive layer to bind the gold to the glass.) The procedure used to deposit the chromium and gold involves mounting four slides on a rotation stage in a vacuum deposition chamber. After bringing the chamber's atmosphere to 2×10^{-6} Torr, a continuous flow of argon (7 ml/min) is introduced into the chamber which enables a chromium layer, approximately 1 nm thick at a rate of 0.01 nm/s, to be deposited by ion sputtering, with the amount of Cr deposited measured by a quartz microbalance mounted above the slides. When the Cr deposition was completed, the argon was shut off and the slides
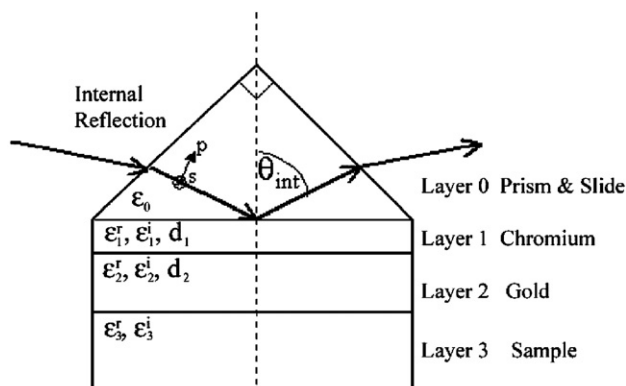
Fig. 3. Schematic showing the light path for internal reflection through a four phase stratified medium.

were allowed to cool as the chamber returned to a minimum pressure. Gold was next deposited on the rotating slides by vapor deposition. Pure gold wire (99.998%) was wrapped onto a thermal resistance wire prior to the evacuation of the chamber. Electricity was slowly applied to the wire, heating the gold to vaporization, until a deposition rate of 0.3 nm per minute was achieved. Deposition was allowed to continue until approximately 50 nm of gold was deposited onto the slides. The slides and chamber were allowed to cool under vacuum for 2 h before the chamber was re-pressurized and the slides removed. Prior to use, the slides were washed a second time in a piranha bath for 5 min, rinsed with water and ethanol, then dried with nitrogen. Finally, the slides were cut into 5 pieces and stored in a desiccator prior to their use.

5.3. Chemicals

Methanol, ethanol, isopropanol, 1-butanol, *t*-butanol, pentanol, hexanol, Nafion (5% solution), methacrylic acid (MAA), *N*,*N*′-methylenebisacrylamide (MBA), and 2, 2-dimethhoxy-2-phenyl-acetophenone (DMPA) were obtained from Aldrich (Milwaukee, WI). *N*-isopropylacrylamide (NIPA) and acetontrile were purchased from Acros (New Jersey, USA). Sodium chloride, potassium chloride, lithium chloride, calcium chloride, lead nitrate, and copper chloride were obtained from Baker. High purity water was purchased from EM Science (Merck KGaA, Darmstadt, Germany). Ruthenium (II) trisbipyridine chloride hexahydrate was obtained from Aldrich. All reagents and solvents were used as received.

Deionized water from a reverse osmosis purification system was used to prepare all ruthenium (II) trisbipyridine chloride solutions. These solutions were prepared by placing an appropriate amount of ruthenium (II) trisbipyridine chloride into a volumetric flask and filling the volumetric flask to the mark with deionized water. Stock solutions of sodium chloride, potassium chloride, lithium chloride, calcium chloride, lead nitrate, and copper chloride were prepared with deionized water and then diluted to the appropriate concentration using deionized water.

Polymer microspheres of *N*-isopropylacrylamide-methacrylic acid (polyNIPA-MAA) were synthesized by free radical dispersion polymerization. In a typical synthesis, NIPA (14 mmol), methacrylic acid (2 mmol), MBA (2 mmol), and DMPA (0.2 g) were transferred to a 500 ml 3-neck round bottom Pyrex flask and dissolved in 100 ml acetonitrile. The monomer solution was sonicated using a Branson 1510 ultrasonicater and purged with dry nitrogen gas for 20 min in order to remove dissolved oxygen. Free radical photoreaction was performed at room temperature in a Rayonet photoreactor equipped with G4T5 type mercury lamps and a cooling fan. After a 12 h reaction period, a turbid polymer suspension was transferred into two 50 ml polypropylene centrifuge tubes and centrifuged at 3000 RPM for 10 min. After separating the decant, the particles were resuspended in 25 ml aliquots of 90/10 (v/v) mixture of methanol and glacial acetic acid, sonicated for 30 min and centrifuged at 3000 RPM for 10 min. This washing procedure was repeated four times in

order to remove unreacted reagents. Finally, the particles were washed 3 times with 25 ml aliquots of methanol, resuspended in a small amount of methanol and stored in glass vials until they were used.

6. Results and discussion

6.1. Refractive indices of short and medium chained length alcohols

Using a gold-coated SF10 slide, the refractive indices of solutions can be directly measured. The first measurement should be performed in air to determine the dielectric properties and thickness of the metal layers on the SF10 slide. This should be followed by ultra pure water to establish the accuracy of the instrument or to determine if re-alignment is needed. Once the physical constants of the metal layers are known, refractive index studies of liquids can be undertaken.

SPR spectra obtained from water and a series of pure organic solvents (methanol, ethanol, 2-propanol, 1-butanol, 1-pentanol, and 1-hexanol) are shown in Fig. 4. The spectra were obtained at ambient temperature. As the molecular weight of the alcohol increases, the resonance angle also increases, which is the expected behavior since the resonance angle increases with increasing refractive index of the solution in contact with the gold layer. Because the refractive index of small and medium chained length alcohols increases as the molecular weight of the alcohols increases, the SPR spectra shown in Fig. 4 are following the anticipated trend.

Once the data had been collected, they were analyzed using the MATLAB modeling program. Starting with the bare sample slide, the dielectric coefficients and thickness of the gold and chromium layers were determined in air. Each sample spectrum was then fitted to a 4-layer model (layers 0, 1, 2, and 3) using the gold and chromium values found in the previous (air) spectrum for thickness and dielectric constants of layers 1 and 2. For each sample, the dielectric coefficients c (ε_r, ε_i) computed were then converted to the absolute index of refraction (ç) using Eqs. (1) and (2) where ε_r and ε_i are the real and imaginary values of the
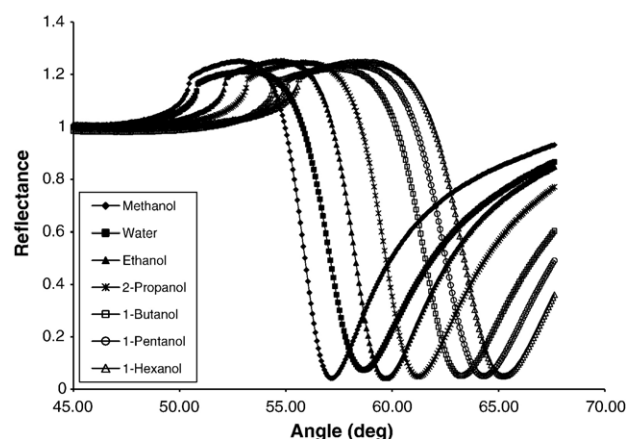
Fig. 4. SPR spectra of methanol, water, ethanol, 2-propanol, 1-butanol, 1-pentanol, and 1-hexanol using an SF-10 glass prism and SF-10 glass slide.
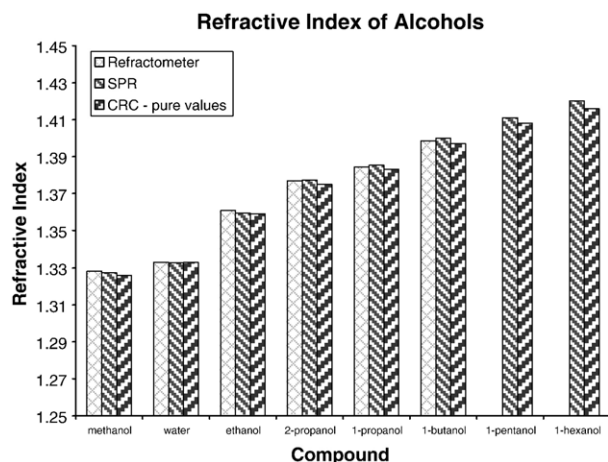
Fig. 5. Comparison of refractive index values for methanol, water, ethanol, 2-propanol, 1-butanol, 1-pentanol, and 1-hexanol using the literature values (Handbook of Chemistry and Physics), SPR, and a digital refractometer. The refractive index values of pentanol and hexanol lie outside of the range of values that can be reliably measured by the digital refractometer.

dielectric constant and ε is the dielectric constant of the third layer which is the liquid in direct contact with the gold.

$$\varepsilon = \left(\varepsilon_r^2 + \varepsilon_i^2\right)^{1/2} \tag{1}$$

$$\eta = \left(\varepsilon\right)^{1/2} \tag{2}$$

Fig. 5 compares the refractive index values computed from each SPR spectrum to those values obtained by a digital refractometer (SPER Scientific Digital Refractometer 300024) and to the reported values found for the same compounds in the Handbook of Chemistry and Physics [16]. For pentanol and hexanol, the refractive indices lie outside the range of values that can be reliably measured by the digital refractometer, which is our reason for not reporting them. For methanol, water, ethanol, 2-propanol, *t*-butanol, and 1-butanol, the differences in the refractive indices reported by these two instruments lie within their experimental error (0.0005 for the SPR instrument and 0.00013 for the digital refractometer at ambient temperature.) For the SPR instrument, the uncertainty was determined by fitting three SPR curves obtained for distilled water and computing the standard deviation of the fitted values obtained for the refractive index. The uncertainty for the digital refractometer was obtained directly from the manufacturer.

6.2. Absorption rates of Nafion

Because polymers are ideal materials to form thin films on substrates (such as on SPR slides), and their optical properties often change upon interaction with other molecules, SPR can be used to study the partition of molecules into polymer films. By coating a film of Nafion onto a gold surface, the partitioning of a compound into a thin film can be studied. For this reason, Nafion (a polymer with negative charge) and ruthenium (II)

trisbypridine chloride hexahydrate (a positively charged complex) were chosen as a model system to study. Seliskar [17,18] has used ruthenium (II) trisbipyridine chloride as a probe to investigate the partitioning of compounds into Nafion. Because the absorption rate of the ruthenium complex is on the minute time scale, this system is ideally suited for study by SPR. Our interest in studying Nafion is also motivated by its use in fuel cells for ion transfer. Compounds that are absorbed by Nafion can alter its ion transfer properties.

To prepare a gold slide for this experiment, it was necessary to coat Nafion onto the slide. This was achieved by spin coating the Nafion onto the gold using a Laurell Technology Corporation Model WS-400B-6NPP/LITE/8K spin coater. Five drops of a 2% Nafion solution was placed on a slide which was then rotated for 5 s at 500 rpm and then for 25 s at 3000 rpm. The slide was then allowed to dry before use. Once the slide was dry, the glass face of the sample slide was cleaned with a Kimwipe and ethanol. After cleaning, the slide was mounted into the SPR flow cell. Distilled water was added to the flow cell for 1 h to hydrate the membrane.

An initial spectrum was taken of the slide with distilled water as the reference. Water was removed from the flow cell and 9 ml of an aqueous solution of 1×10^{-5} M ruthenium (II) trisbipyridine chloride was injected into the flow cell at a rate of 0.1 ml/min using a syringe pump. An SPR spectrum was taken every 5 min for approximately 1 h, with the first spectrum taken immediately with the start of the syringe pump. After each spectrum was collected, the optical alignment of the prism and the primary detector was checked as small changes in alignment can occur.

Fig. 6 shows a plot of the refractive index versus time obtained from SPR spectra collected for the 1×10^{-5} M ruthenium (II) trisbipyridine chloride solution. The refractive
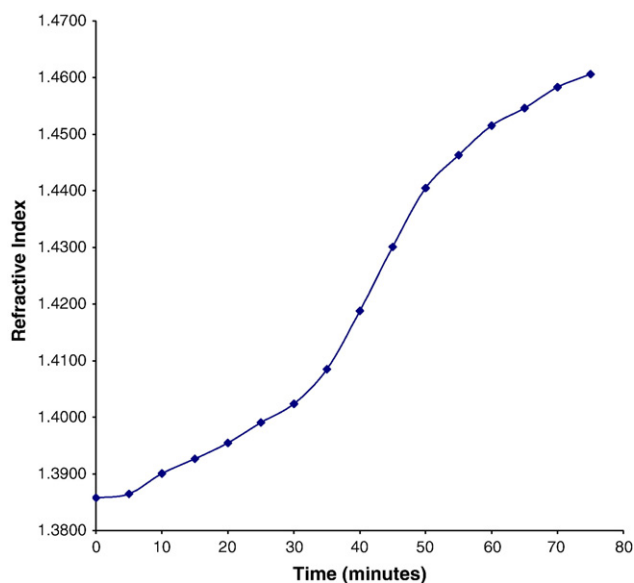
Fig. 6. A plot of the refractive index versus time using spectra collected for 1×10^{-5} M ruthenium (II) trisbipyridine chloride. The MATLAB modeling program developed in house was used to compute the refractive index of the Nafion layer from the SPR spectra.

Absorption of Ru Complex in a Nafion Film
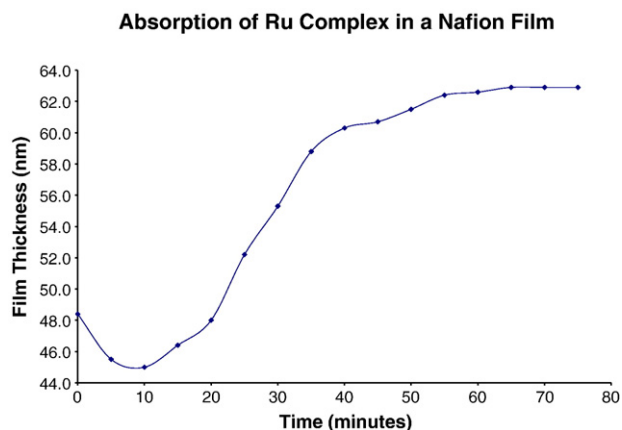
Fig. 7. A plot of the Nafion film thickness versus time using spectra collected for 1×10^{-5} M ruthenium (II) trisbipyridine chloride. The MATLAB modeling program developed in house was used to compute the film thickness of the Nafion layer from the SPR spectra.

index of the Nafion layer increases over time due to the uptake of ruthenium (II) trisbipyridine chloride. On the other hand, the thickness of the Nafion film initially decreases with ruthenium uptake (see Fig. 7) indicating that contraction of the film has occurred. The MATLAB modeling program was used to compute both the refractive index and thickness of the Nafion layer from the SPR data using a 5-layer model (Layers 0, 1, 2, 3, and 4). For the fitting, the refractive index of distilled water was used for the ruthenium solution in contact with the Nafion membrane since the concentration of the analyte was judged not to be sufficiently high to change the refractive index of water. The thickness of the Nafion film in water prior to the start of the uptake was determined to be approximately 48 nm. After an initial period of contraction, the film began to expand, surpassing its initial thickness after 20 min (see Fig. 7). Because the refractive index of the film is increasing over time (see Fig. 6), the contraction initially experienced by the film is probably due to expulsion of water caused by the initial uptake of ruthenium (II) trisbipyridine chloride. Interestingly enough, Zudans et al. [18] reported very similar results even though he used Nafion films of different thicknesses (438 nm versus 48 nm) and employed ellipsometry (in lieu of SPR) to characterize his films.

6.3. Adsorption of metal ions by polyacrylamide hydrogels

Hydrogels prepared from *N*-isopropylacrylamide (NIPA) have received considerable attention in the scientific literature because of the large volume change which these materials undergo in response to an external stimulus such as temperature or pH [19–21]. PolyNIPA hydrogels will suddenly go from a swollen state to a shrunken state at 32 °C. For this reason, hydrogels prepared from NIPA have been applied in thermosensitive drug delivery systems [22] and separation processes [23]. The reversible volume phase transition that polyNIPA gels undergo also makes them an attractive material for removal of pollutants from the environment. Recently, hydrogels prepared

from NIPA have been investigated as potential adsorbents for removal of metal ions in waste water [24]. However, little is known about the adsorption of metal ions by polyNIPA hydrogels [25]. Therefore, SPR was used to study noncompetitive metal ion binding by polyNIPA-MAA particles. In this study, the solutions that were placed in contact with the polymer particles consisted of a metal salt dissolved in distilled water.

Fig. 8 shows a plot of refractive index versus the log of the concentration of Group I and II metal ions (10^{-7} M to 10^{-1} M) obtained from SPR spectra for polyNIPA-MAA particles spin coated onto a gold surface. For spin coating, the polymer particles were dispersed in methanol to prepare a stable suspension. Ten drops of the methanol solution were placed in the center of the sample slide, which was spun at 500 rpm for 5 s and 3000 rpm for 25 s. Two additional drops of the polymer solution were placed on the slide and the spin coating procedure was repeated. This was done two or three times until a nearly uniform layer was formed as determined by visible microscopy using a Leitz Orthoplane microscope.

The refractive index of the polymer particles was determined by fitting the SPR data to a 5-layer model (Layers 0, 1, 2, 3, and 4) with the diameter of the polyNIPA-MAA particles defining the thickness of the third layer. (The diameter of the polyNIPA-MAA particles as determined by scanning electron microscopy is approximately 500 nm and they appear to be monodispersed.) As the concentration of Li^+, Na^+, K^+, or Ca^{++} in contact with the polymer particles increased, the refractive index of the particles decreased due to an increase in the water content of the polymer. Evidently, the presence of these cations in the solution caused the polymer to swell. In all likelihood, the monovalent and divalent cations displace protons from the carboxylic acid groups in the hydrogel via an ion exchange mechanism. Deprotonation of the methacrylic acid groups in the copolymer structure increases the affinity of the polymer for water. As a result, a higher temperature is required for the volume phase transition to occur. Metal ion binding by Group I and Group II cations through ion pairing increases the water content of the polyNIPA-MAA particles. The adsorbed ions act as fix charges
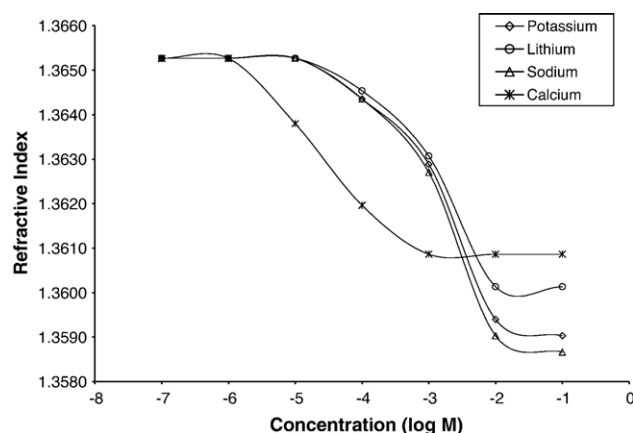
Fig. 8. Refractive index versus the log of the concentration of Na^+, K^+, Li^+, and Ca^{2+} obtained from SPR spectra for polyNIPA-MAA particles spin coated onto a gold surface.

on the network chains raising the lower critical solution temperature of the polymer.

The lack of selectivity exhibited by the polyNIPA-MAA particles towards the group I metal ions can be attributed to the low level of crosslinking used, which allows the particles to swell. Unfortunately, the hydration that occurs because of swelling decreases the density of the binding sites and their selectivity for the different metal ions. This phenomenon which is well known among workers in the field of ion exchange chromatography [26] has been the subject of numerous studies.

The swelling and shrinking behavior exhibited by poly-NIPA-MAA particles in contact with solutions of Pb^{2+} or Cu^{2+} is more complex (see Fig. 9). At low concentrations of Pb^{2+} or Cu^{2+} (e.g., 10^{-7} M and 10^{-6} M), the decrease in refractive index is probably due to an increase in the volume phase transition temperature of the polymer, which can be attributed to deprotonation of the methacrylic acid groups by Pb^{2+} or Cu^{2+} through an ion exchange mechanism. At higher concentrations of Pb^{2+} or Cu^{2+}, the refractive index of the polymer particles increases suggesting that water is being squeezed out of the polymer. We attribute this to Pb^{2+} or Cu^{2+} being bound to both the carboxyl group of MAA by ion exchange and to the nitrogen atom of NIPA through coordination with its lone pair forming a chelate. Pb^{2+} or Cu^{2+} via complexation through coordination and ion exchange is effectively acting as a crosslinker reducing the particle diameter and lowering the affinity of the polymer for the solvent, which is water. Alternatively, the binding of Pb^{2+} or Cu^{2+} to the nitrogen atom of NIPA disrupts the hydrogen bonding between the water molecules and the NH_2 group on the polymer backbone reducing the affinity of the polymer for water. In either case, the refractive index of the polymer would increase, which is consistent with our experimental data.

Previous workers [27] have reported the release of both Pb^{2+} and Cu^{2+} from microgel particles through heating. However, in more recent published work, this was not observed [28,29], which suggests that ion binding capabilities of the polymer are not affected by the collapse of the network structure. We have investigated the release Li^+, Na^+, K^+, Ca^{++}, Pb^{2+} and Cu^{2+} from the microgel particles through acid treatment and have observed that complete desorption of these cations occurs. This is consistent with our hypothesis for the adsorption of alkali, alkaline earth and transition metal ions by the microgel particles.
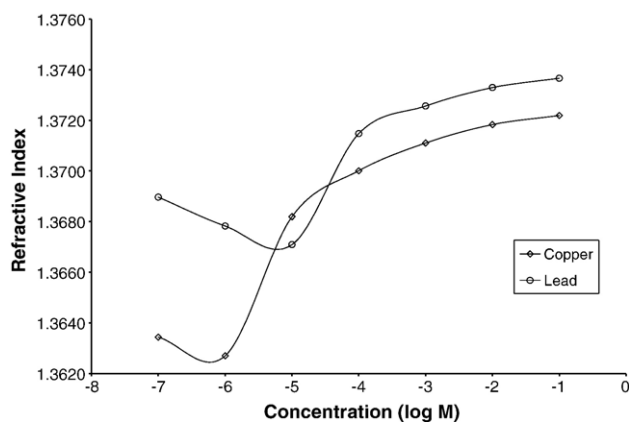
7. Conclusion

The three studies highlighted in the previous section demonstrate the value of the proposed SPR instrument for both teaching and research. In the first study, which can be performed directly in the undergraduate teaching laboratory, a referee method was used to validate the performance of our open platform instrument. As for the second study which involves a current area of active research, this experiment can also be performed in the undergraduate teaching laboratory if dip coating is substituted for spin coating. Dip coating is performed by slowly dipping the sample slide in a dilute solution of Nafion, which can be prepared by adding *n*-propanol to the 2% Nafion solution. Before dipping the slide into the solution, the slide must be clean and dry. If necessary, the sample slide can be washed with deionized water, then ethanol and dried with compressed gas. Using a pair of tweezers, it is a simple matter to quickly dip the slide in a small amount of the Nafion solution followed by removing any excess solution and allowing the slide to dry in a container protected from airborne contaminants. Once dry, the glass side of the gold slide will need to be cleaned with a Kimwipe and ethanol to remove any Nafion. After cleaning, the slide can be mounted onto the prism, with the prism and slide inserted into the instrument. Water can then be added to the sample reservoir for the purpose of hydrating the membrane.

The third study demonstrated the value of an open platform instrument for basic research. Although we prepared our own gold slides in all three studies, the slides can be purchased commercially from a number of vendors. However, the piranha solution, which is used to clean the slides, is hazardous. Care must be taken when using it. Gloves, goggles, and a lab coat are strongly recommended when using the piranha solution due to its corrosive nature. After washing all of the sample slides, the piranha solution should be neutralized and then placed in a waste solvent container bottle that is properly labeled.

A Class IIIA laser is used in the SPR instrument. This designation means that it will not cause blindness unless an individual is subjected to prolonged exposure. Nevertheless, we recommend covering the instrument while it is in use to reduce the likelihood of anyone being exposed to stray laser light.

Fig. 9. Refractive index versus the log of the concentration of Cu^{2+} and Pb^{2+} obtained from SPR spectra for polyNIPA-MAA particles spin coated onto a gold surface.

Appendix A. Supplementary data

Supplementary data associated with this article can be found, in the online version, at doi:10.1016/j.microc.2007.02.003.

References

[1] L.S. Jung, C.T. Campbell, T.M. Chinowsky, S.Y. Yee, Langmuir 14 (1998) 5636.
[2] A.G. Frutos, R.M. Corn, Anal. Chem. 70 (1998) 449A.
[3] E. Garcia Riuz, I. Garces, C. Aldea, M.A. Lopez, J. Mateo, J. Alonso-Chamarro, S. Alegret, Sens. Actuators, A 221 (1993) 37.
[4] K. Alfthan, Biosens. Bioelectron. 13 (1998) 653.
[5] J. Homola, S.Y. Lee, G. Gauglitz, Sens. Actuators, B B 54 (1999) 3.
[6] H. Gu, Z. Ng, T.C. Deivaraj, X. Su, K.P. Loh, Langmuir 22 (8) (2006) 3929.
[7] R. Mukhopadhyay, Anal. Chem. 76 (15) (2005) 313A.
[8] L.S. Miller, M.B. Nakhleh, J.J. Nash, J.A. Meyer, J. Chem. Ed. 81 (2004) 1801.
[9] E. Kretschmann, H. Raether, Z. Naturforsch. 23 (1968) 2135.
[10] B. Liedberg, C. Nylander, I. Lundstrom, Biosens. Bioelectron. 10 (1995) i.
[11] A.Z. Otto, Phys. Status Solidi 26 (2) (1968) K99.
[12] J. Homola, I. Koudela, S. Yee, Sens. Actuators, B, Chem. B54 (1–2) (1999) 16.
[13] R. Slavik, J. Homola, J. Ctyroky, E. Brynda, Sens. Actuators, B, Chem. B74 (1–3) (2001) 106.
[14] Y.-C. Kim, J.-F. Masson, K.S. Booksh, Talanta 67 (5) (2005) 908.
[15] L.A. Obando, D.J. Gentleman, J.R. Holloway, K.S. Booksh, Sens. Actuators, B, Chem. B 100 (3) (2004) 439.
[16] R.C. Weast (Ed.), Handbook of Chemistry and Physics, 70th edition, CRC Press, Boca Raton, FL, 1990.
[17] N. Kaval, C.J. Seliskar, W.R. Heineman, Anal. Chem. 75 (22) (2003) 6334.
[18] I. Zudans, W.R. Heineman, C.J. Seliskar, J. Phys. Chem. B 108 (2004) 11521.
[19] T. Tanaka, Phys. Rev. Lett. 40 (1978) 820.
[20] S. Hirotsu, Y. Hirokawa, T. Tanaka, J. Chem. Phys. 87 (2) (1987) 1392.
[21] H. Kawasaki, A. Sasaki, H. Maeda, J. Phys. Chem., B 101 (1997) 5089.
[22] M. Kawashima, H. Katano, K. Sanui, N. Ogata, T. Okano, Y. Sakurai, Macromolecules 27 (1994) 947.
[23] R.P.S. Freites, E.L. Cussler, Chem. Eng. Sci. 42 (1987) 97.
[24] T. Saitoh, F. Satoh, M. Hiraide, Talanta 61 (2003) 811.
[25] G.E. Morris, B. Vincent, M.J. Snowden, J. Colloid Interface Sci. 190 (1997) 198.
[26] O. Shipigun, Y.A. Zolotov, Ion Chromatography in Water Analysis, Ellis Horwood Limited, Chichester, 1988.
[27] M.J. Snowden, D. Thomas, B. Vincent, Analyst 118 (1993) 1367.
[28] J. Lehto, K. Vaaramaa, E. Vesterinen, H. Tenhu, J. Appl. Polymer Sci. 68 (1998) 355.
[29] K. Yamashita, T. Nishimura, M. Nango, Polym. Adv. Technol. 14 (2003) 189.